IEEE Access
Multidisciplinary | Rapid Review | Open Access Journal

Received 15 April 2023, accepted 17 May 2023, date of publication 23 May 2023, date of current version 1 June 2023.

Digital Object Identifier 10.1109/ACCESS.2023.3279131

APPLIED RESEARCH

Small-Sized Immersible Water Heaters for Domestic Induction Heating Technology

ALBERTO PASCUAL[1], (Graduate Student Member, IEEE), JESÚS ACERO[1], (Senior Member, IEEE), SERGIO LLORENTE[2], CLAUDIO CARRETERO[3], (Senior Member, IEEE), AND JOSÉ M. BURDIO[1], (Senior Member, IEEE)

[1]Department of Electronic Engineering and Communications, University of Zaragoza, 50018 Zaragoza, Spain
[2]Department of Research and Development, Bosch-Siemens Home Appliances Group, 50016 Zaragoza, Spain
[3]Department of Applied Physics, University of Zaragoza, 50009 Zaragoza, Spain

Corresponding author: Alberto Pascual (a.pascual@unizar.es)

This work was supported in part by the Spanish MCIN/AEI/10.13039/501100011033 co-funded by EU through NextGenerationEU/PRTR and FEDER Programs under Project PID2019-103939RB-I00, Project PDC2021-120898-I00, and Project CPP2021-008938; in part by the DGA-FSE; and in part by the BSH Home Appliances Group.

ABSTRACT Induction cooktops are a key element in home electrification. This paper presents a new use of induction cooktops, which allows the preparation of infusions directly in a ceramic mug. It is proposed the design of a water heater with an immersible metallic load. The dimensions of the load allow its embedding in small ceramic vessels. Despite being smaller than conventional inductors, the immersible load has a specific shape that allows it to efficiently receive the energy from the induction cooktops and quickly heat the liquid inside the mug. Its geometry consists of a flat disk with sidewalls on its edge, which provides low reluctance paths for the magnetic field, resulting in improved transmitted power and efficiency. The load is arranged in a multilayer structure consisting of a ferromagnetic alloy with low Curie temperature at the bottom and aluminum on the top, which confers self-detection capabilities against dangerous overheating. The study of the proposal has been carried out with a finite element analysis model, and the feasibility of this proposal has been demonstrated through experimental results of its performance. Finally, the immersible water heater, powered by an induction cooktop, has been compared to other liquid heating systems, such as the microwave and the kettle, with promising results.

INDEX TERMS Home appliances, induction heating, magnetic devices, electromagnetic induction.

I. INTRODUCTION

Induction heating (IH) provides contactless, fast, and efficient heating of conductive materials. Its application in a domestic scenario is widely used in commercial applications and is an active research field with numerous contributions and improvements. In recent years, IH cooktops have become more efficient [1], [2], safer [3], cleaner, faster, and easier to use [4], as well as more flexible in terms of cooking surface [5], [6] and cookware materials [7], [8], [9], [10].

The associate editor coordinating the review of this manuscript and approving it for publication was Guido Lombardi.

An induction cooktop usually comprises the power electronic converter, the control unit, and the inductor-load system [11]. Induction cooktops take power from the mains voltage, rectified by a complete diode bridge. This is followed by a bus filter designed to allow a large voltage ripple resulting in an input power factor close to one. Then, the resonant inverter supplies an alternating current between 20-100 kHz to the inductor. Due to the balance between cost, ease of implementation, and performance, the most widely used inverter in domestic IH is the half-bridge topology [12]. Lastly, the coil generates an alternating magnetic field in which the heating target, the ferromagnetic load, is immersed. As a result, two physical phenomena heat the load: eddy

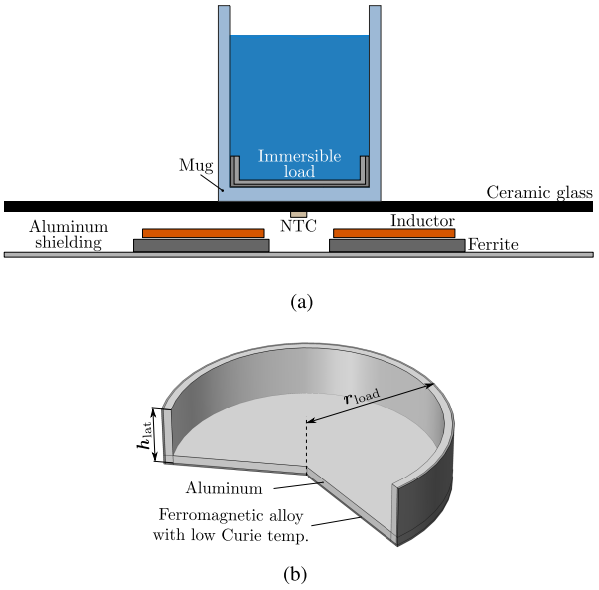

FIGURE 1. Representation of the immersible heater load powered by an induction cooktop (a) and its geometry and materials (b).

currents and magnetic hysteresis [13]. Eddy currents oppose the applied magnetic field of the load and produce heat due to the Joule effect, which is usually the main heat source in induction heating processes. In addition, magnetic hysteresis creates additional heating in ferromagnetic materials.

Among all the advantages of induction heating technology [14], its high efficiency stands out, making it highly suitable for promoting the efficient electrification of homes. As a result, new uses for this technology are emerging, such as its application to the development of small wireless appliances (cooking robots, rice cookers) that can be powered from an induction cooktop [15], [16]. Compared to others, the efficiency and speed of this technology are currently desirable for any food or liquid (water, milk) heating process.

Preparing tea and coffee is one of the most recurrent processes in every household. The preferred solution for preparing infusions is to use a kettle that quickly provides a high-quality infusion. However, it is usually a bulky instrument that requires some time for preparation and cleaning, as well as storing space. In addition, a survey of 86,000 British households by the Energy Saving Trust [17] found that three-quarters of households admitted to overfill the kettle when boiling water. It is estimated that, on average, the kettle wastes about 15% of the energy used and the water heated due to water overfilling [18]. Another product used to prepare infusions is the microwave oven. Some users choose it over the kettle because the infusion preparation process is more convenient. However, it is slower, has an uneven heat distribution that worsens the final quality of the infusion [19], and is less efficient, since microwave ovens typically have a conversion efficiency from electrical mains to microwave energy close to 50% [20].

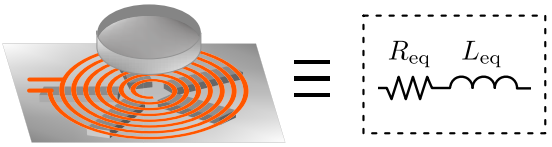

FIGURE 2. Equivalent circuit of the induction system.

This paper proposes the water heater with an immersible load for domestic IH systems depicted in Fig. 1(a). It can be embedded or built into a ceramic mug and combines the convenience of the microwave with the temperature uniformity and efficiency of the kettle. In addition, it requires little space for storage and allows the preparation of the infusion directly in the cup where it is to be consumed, making the process more convenient for daily use.

The design of this inductive water heater has to cope with three main problems. The immersible load has to fit in a standard mug; therefore, its size is much smaller than that of conventional inductors. In addition, the distance between the inductor and the load is increased since it is added the mug base height. These two factors disperse the magnetic fields and consequently decrease the transmitted power and efficiency considerably [21]. For this reason, it is proposed the load geometry shown in Fig. 1(b), consisting of a disk with sidewalls made of a ferromagnetic material with low Curie temperature at the base united with a layer of aluminum on the upper part. The walls on the edges of the load facilitate low reluctance paths to the magnetic field and increase the efficiency and power delivered to it. Lastly, the heating system should incorporate an overheating detection mechanism to prevent the load from reaching dangerous temperatures in the event of liquid depletion. The materials chosen in the load design provide this protection system [3]. In induction heating, overtemperature can be detected without additional sensors by using a multilayer load design, such as the one shown in Fig. 1(b). This design causes changes in the equivalent impedance of the inductor-load system at a predefined temperature, which, can be automatically detected by the induction cooktop. The validation of the proposal has been carried out at a theoretical level by analyzing its electrical efficiency, and its overall performance has been validated experimentally by means of a prototype. In addition, the system has been compared to the microwave and the kettle, as they are the most commonly used appliances for heating liquids at home.

The paper is organized as follows. Section II is focused on describing the finite element model and the calculation of the system efficiency. Section III shows the technical problems of the inductive water heater and how they have been solved. Section IV and V describe the experimental setup and show the results. Finally, in Section VI, some conclusions are drawn.

II. FINITE ELEMENT MODELING AND INDUCTION EFFICIENCY

To evaluate the performance of an induction heating system is essential to know the distribution of electric and magnetic fields in it. For this purpose, the system has been electromagnetically modeled using the finite element analysis tool COMSOL. The model is based on Fig. 1(a) and consists of the ferromagnetic load, whose geometry and size are adapted to this specific situation, under which are placed, from top to bottom, the planar inductor, the flux concentrators (ferrites) to improve the coupling, and the aluminum shielding that protects the electronics located below the inductor. The model employs 3D geometry and has been used to study different load shapes in order to optimize the efficiency and the power dissipation for size-constrained situations. The finite element model has been developed considering the following simplifications:

- The multiturn winding composed of an intricate Litz wire is replaced by an ideal constant current density J of a rectangular cross-section area S_{coil}.
- Materials are linear, homogeneous, and isotropic and are characterized through their electrical conductivity σ and the relative magnetic permeability μ_r.
- The thickness of the aluminum shielding is assumed to be greater than the skin depth at the operating frecuency. The skin depth determines the effective area through which current flows in a conductor. Thus, this element can be replaced by an impedance boundary condition (IBC) provided by the FEA tool COMSOL.

The induction system, illustrated in Fig. 2, can be electrically modeled by an equivalent impedance (Z_{eq}), which is defined as the ratio of the voltage (V_{coil}) and the current in the coil (I_{coil}). The voltage is obtained by integrating the electric field over the entire volume of the coil divided by its cross-sectional area S_{coil} and multiplied by the number of turns n_t [22]. Considering that the inner and outer radii of the coil are r_{int} and r_{ext} respectively, and the thickness of the coil is t_w, it is obtained that:

$$V_{coil} = -\oint Edl = -\frac{n_t}{S_{coil}} \int_{r_{int}}^{r_{ext}} \int_0^{t_w} 2\pi r E_\varphi dz dr \tag{1}$$

$$Z_{eq} = \frac{V_{coil}}{I_{coil}} = R_{eq} + jwL_{eq} \tag{2}$$

where w is the angular frequency and E_φ is the electrical field in the coil. The Z_{eq} has a real part R_{eq}, which represents the total power dissipated in the system, and an imaginary part L_{eq}, which represents the magnetic field of the system. Consequently, the power factor is determined as follows:

$$PF = \frac{R_{eq}}{|Z_{eq}|} \tag{3}$$

Two parameters characterize the performance of an induction heating system: the load equivalent induced resistance R_l, which represents the power dissipated in the load, and the induction efficiency η_{ind} [23]. According to the ideal current density model of the coil, the R_l together with the dissipation in the ferrites and the aluminum shielding, R_{sh}, constitutes the R_{eq}. However, for the calculation of the system efficiency, it must be taken into account that the measured R_{eq} in the real system also includes the winding losses, R_w. The R_l and R_{sh} can be obtained by integrating the flux of the Poynting vector S at the load and shielding boundaries, respectively. Considering normalized fields per Ampere $\overline{\mathrm{E}} = \mathrm{E}/\hat{I}_{coil}$, $\overline{\mathrm{H}} = \mathrm{H}/\hat{I}_{coil}$, these resistances can be expressed as follows:

$$R_\alpha = Re\left[\int_{S_\alpha} [(\overline{\mathrm{E}} \times \overline{\mathrm{H}}^*) \cdot \hat{n}] dS_\alpha\right] \quad \alpha = l, sh \tag{4}$$

where $\hat{n}$ is the normal vector to the load or shielding surface and S_α is the area of the corresponding surface. The winding losses can be divided into those caused by dc, and skin effect, R_{cond}, and those caused by the magnetic field's proximity losses, R_{prox}. It has been considered that the coil is wounded with n_t turns of Litz wire with n_s strands of radii r_s. In addition, it has been taken the approximation that the strands are equivalent and are placed at the position of the mean length of turn (MLT $= \pi(r_{ext} + r_{int})$). Consequently, R_{cond} is calculated as follows [24]:

$$R_{cond} = \frac{n_t}{n_s} \frac{\mathrm{MLT}}{\sigma_w(\pi r_s^2)} \Phi_{\mathrm{cond}}\left(\frac{r_s}{\delta}\right) \tag{5}$$

where σ_w is the electrical conductivity of the strand, δ is the skin depth, and $\Phi_{\mathrm{cond}}(r_s/\delta)$ is the ac resistance of a strand per unit of length. The skin depth can be obtained by meas of:

$$\delta = \sqrt{1/(\pi f \mu_0 \mu_r \sigma)} \tag{6}$$

being f the operation frequency, μ_0 the magnetic permeability of vacuum and σ and μ_r the electromagnetic properties of the medium. In addition, since the coil is immersed in a variable magnetic field, proximity losses are also generated. The proximity losses of the conductors in windings are proportional to the length of the conductor multiplied by the squared amplitude of the external magnetic field over the conductor. This can be approximated by the spatial average of the norm of the magnetic field in the coil volume generated by one turn placed in the MLT position [25]:

$$\langle|\overline{\mathrm{H}}^2|\rangle = \frac{n_t^2}{S_{coil}} \int_{V_{coil}} |\overline{\mathrm{H}}^2_{\mathrm{p.t.}}| dV_{Coil} \tag{7}$$

$$R_{prox} = n_s n_t \frac{4\pi}{\sigma_w} \Phi_{\mathrm{prox}}\left(\frac{r_s}{\delta}\right) \langle|\overline{\mathrm{H}}^2|\rangle \tag{8}$$

where V_{coil} is the volume of the coil. $\Phi_{\mathrm{prox}}(r_s/\delta)$ takes into account the ac dependence on the proximity losses of the strand; for cases where $r_s/\delta \leq 1$ it can be approximated by [26]:

$$\Phi_{\mathrm{prox}}\left(\frac{r_s}{\delta}\right) \approx \frac{1}{4}\left(\frac{r_s}{\delta}\right)^4 \tag{9}$$

Finally, the induction efficiency is the ratio of the power delivered into the load with respect to the electrical power supplied to the coil. It is usually be represented by the following relationship between resistances:

$$\eta_{ind} = \frac{R_l}{R_l + R_{sh} + R_{cond} + R_{prox}} \tag{10}$$

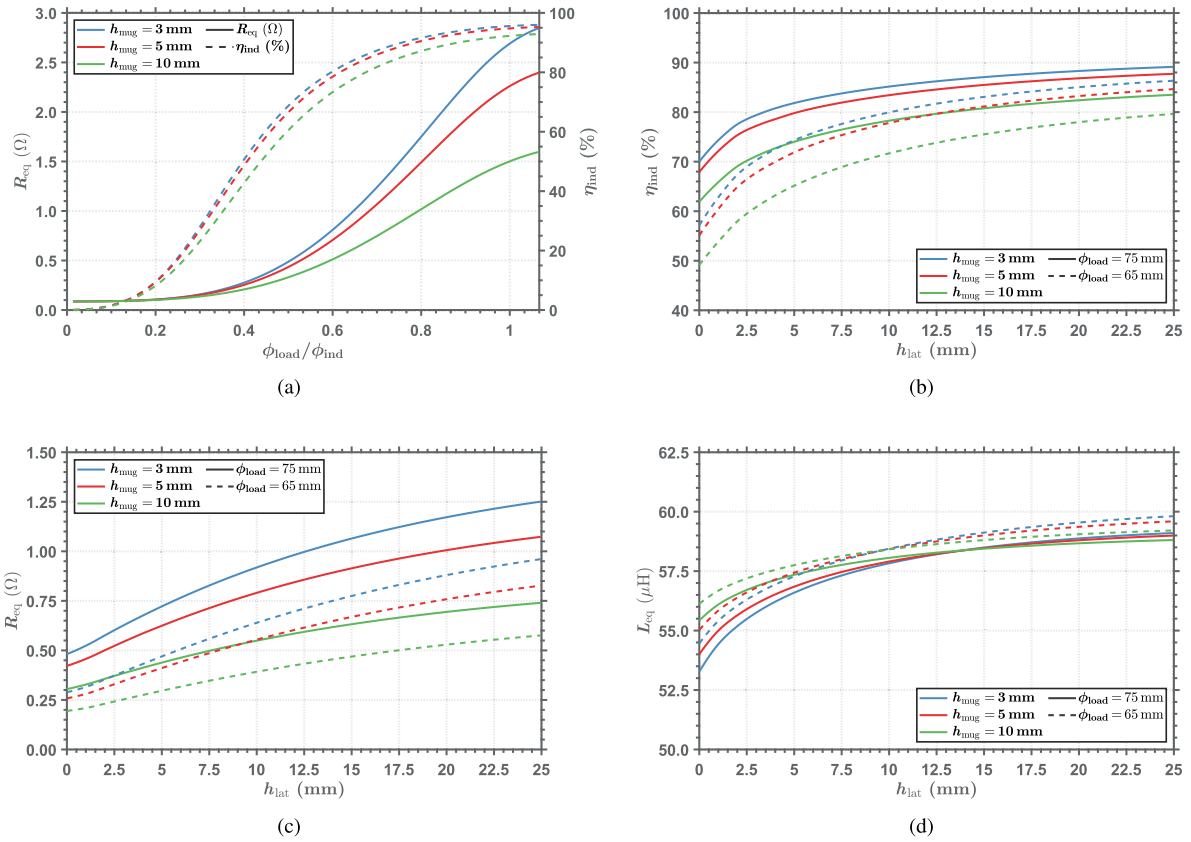

FIGURE 3. Simulation results at f=30 kHz for various load geometries when immersed in mugs with different base heights (h_{mug}). Efficiency and R_{eq} as a function of the load/inductor size ratio (a). η_{ind} (b), R_{eq} (c), and L_{eq} (d) with respect to the height of the load lateral wall (h_{lat}) in a inductor-load system with ϕ_{ind} = 150 mm and ϕ_{load}= 65-75 mm.

III. ANALYSIS AND DESIGN OF INDUCTIVE HEATERS FOR NON-METALLIC SMALL-SIZE COOKWARE

As it was above commented, three main challenges were faced in the design of the solution presented in Fig. 1: the reduced ferromagnetic load size with respect to the inductor, the increased distance between the inductor and the load, and the overheating protection. The induction system analysis has been performed using the finite element model described above. The system consists of a commercial circular coil with an external diameter of 150 mm and an internal diameter of 45 mm, wound with 24 turns of Litz wire of 32 strands with a diameter of 0.3 mm each. In addition, the coil incorporates five equiangularly arranged ferrite bars underneath. The mugs, as they are made of ceramic materials, do not directly interfere with the induction heating process. However, it should be noted that the distance between the load and the inductor comprises a fixed part which is the distance between the inductor and the top surface of the ceramic glass, and a variable part which depends on the height of the base of the mug, h_{mug}, in which the load is embedded above.

A. ADAPTATION OF THE LOAD GEOMETRY

As mentioned above, one of the requirements of this application is that it must fit inside the mug, and, therefore, its diameter should not exceed 70-80 mm. However, as can be seen in Fig. 3(a), the smaller the load size compared to the inductor's size, the lower the efficiency and power dissipation in the system. To compete with other liquid heating systems, the excellent efficiency of induction systems must be maintained and the equivalent resistance must be sufficient to rapidly heat the liquid.

The main problem when the load covers a low percentage of the inductor is that a part of the magnetic field flux, depending on the percentage of uncovered area, is not captured by the load and, therefore, the induced currents and the surface of the load where the power is dissipated is small. In addition, the magnetic field directed towards the aluminum shielding and ferrites is higher, increasing the R_{sh} and the system losses. These effects are further increased when an additional distance is added between the inductor and the load, as in the case of the height of the mug base, h_{mug}, which causes the magnetic fields to spread out more. For these reasons, this work proposes the geometry shown in Fig. 1(b). It consists of a disk with a reduced diameter of 65 mm and 75 mm, which allows it to be inserted into a mug. This disk incorporates lateral walls at the edge to facilitate low reluctance paths for the magnetic field directing it towards the load, allowing more power to be dissipated more efficiently.

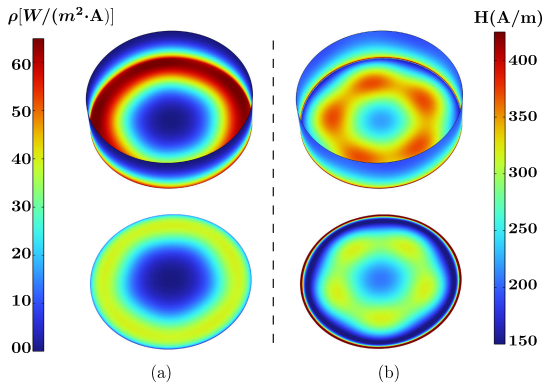

FIGURE 4. Power dissipated per unit current (a) and magnetic field strength (b) in the 20 mm sidewall load and the planar load. Both with a diameter, ϕ_{load}, of 75 mm.

Fig. 3(b) shows how the efficiency of the inductor-load system (ϕ_{ind} = 150 mm, ϕ_{load} = 65-75 mm) increases as the height of the lateral wall (h_{lat}) does. The η_{ind} stabilizes at the wall height of 20 mm where an increase in efficiency of 17% and 29% is achieved in loads with diameters of 75 and 65 mm embedded in a mug with h_{mug} = 5 mm. It can also be seen in Fig. 3(c) how the power that can be dissipated increases as the h_{lat} does. The disk with the 20 mm sidewall receives more than twice the power it receives with a planar disk (h_{lat} = 0 mm). Moreover, Fig. 3(d) shows how the system becomes more inductive as the lateral wall increases. As already mentioned, since the ferromagnetic load is located above the base of the mug, it can be observed in all the graphs that the performance of the system worsens when used in mugs with higher base height (h_{mug}), since the distance between inductor and load increases.

The effect of the sidewalls on the power dissipated per unit of current and the magnetic field strength can be seen in Fig. 4. It shows the difference between the disk with 20 mm of lateral walls and the planar disk, both with a diameter of 75 mm and powered by an inductor of 150 mm diameter. It can be seen in Fig. 4(a) that although most of the power dissipation occurs at the base of the load, the inclusion of the lateral walls provides a low reluctance path for the magnetic fields, which allows the total power dissipation throughout the load to almost double. Similarly, it can be seen from Fig. 4(b) that the incident magnetic field strength at the load's surface also increases significantly with the incorporation of lateral walls. In contrast, in the planar load, the magnetic field tries to concentrate at the edge of the load. The effect of the five ferrites existing in the commercial inductor system can be also appreciated in the shape of the field.

Finally, it is worth mentioning that the special geometry of the load allows to attract the magnetic field lines avoiding field dispersion and Radiated Emission (RE) problems. According to [27] when the distance between the load and the inductor is small, less than 30 mm, the near field emission is not so high as to compromise the standard IEC 62233 [28].

B. SELF-PROTECTION METHOD AGAINST OVERTEMPERATURE

Another technical problem with the proposed water heater is that the overtemperature protection system currently incorporated in induction cooktops is designed for the case of the cookware in contact with the ceramic glass [29]. In commercial cooktops the cookware temperature is estimated from the temperature measurements of an NTC, which, as seen in Fig. 1(a), is located below the ceramic glass. Therefore, the mug adds an extra thermal resistance and consequently the overtemperature protection system does not work correctly. Thus, it is necessary to incorporate a feature that protects the user and the system from possible damage due to overheating the load; as the temperature can increase considerably when there is no liquid or the liquid has evaporated completely.

The method for self-detection of overtemperature in induction heating proposed by [3] is employed to solve this issue. It uses a multilayer load structure with aluminum on the top and a layer with a specific thickness of 0.5 mm with a ferromagnetic alloy with low curie temperature for the bottom. The Curie temperature is the temperature at which a ferromagnetic material becomes paramagnetic, losing its magnetism. This multilayer load presents two different states: a normal state, in which it can be heated efficiently, and a protection state, above the Curie temperature, in which the power factor decreases abruptly, limiting overheating and making this state easily detectable by the cooktop.

The principle of the self-protection method is shown schematically in Fig. 5. On the one hand, it shows the variation of the relative magnetic permeability μ_r with the temperature of the material chosen for the bottom layer, which is an alloy, analyzed in [30], of $Fe_{40.3}Ni_{49}Cr_{10.3}Mn_{0.44}$ with a Curie temperature of 230°C and an electrical conductivity σ of $1{\cdot}10^6$ S/m. On the other hand, it shows the variation of the skin depth as the temperature changes. It is observed that for temperatures below the Curie temperature, the magnetic field does not overpass the ferromagnetic alloy layer, allowing it to heat up efficiently. However, when this temperature is exceeded, the magnetic field reaches the aluminum layer. Since aluminum is non-ferromagnetic and a good conductor, this causes considerable change in the power factor of the equivalent circuit [31]. The changes in the equivalent circuit are constantly monitored by the vessel autodetection system incorporated in commercial cooktops [32], [33]. This system is built into all induction cooktops and stops transmitting power when it detects loads made of non ferromagnetic materials, such as copper or aluminum, whose equivalent PF is low. It should be noted that when the low T_{Curie} alloy cools down, it recovers its original magnetic permeability and can be reheated normally [30].

IV. PROTOTYPE AND EXPERIMENTAL SETUP

The inductive water heater performance has been tested with a commercial induction cooktop composed of a half-bridge series resonant inverter with a resonance capacitor C_r = 540 nF. The electrical circuit diagram of the application is

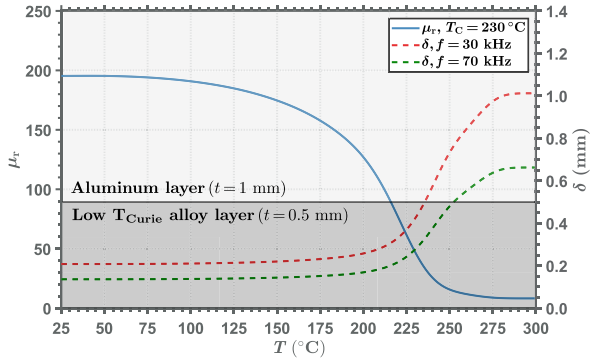

FIGURE 5. Variation with the temperature of the skin depth and the μ_r of the alloy chosen for the bottom layer ($T_{Curie} = 230$°C).

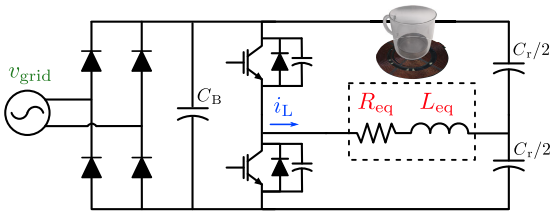

FIGURE 6. Experimental circuit diagram.

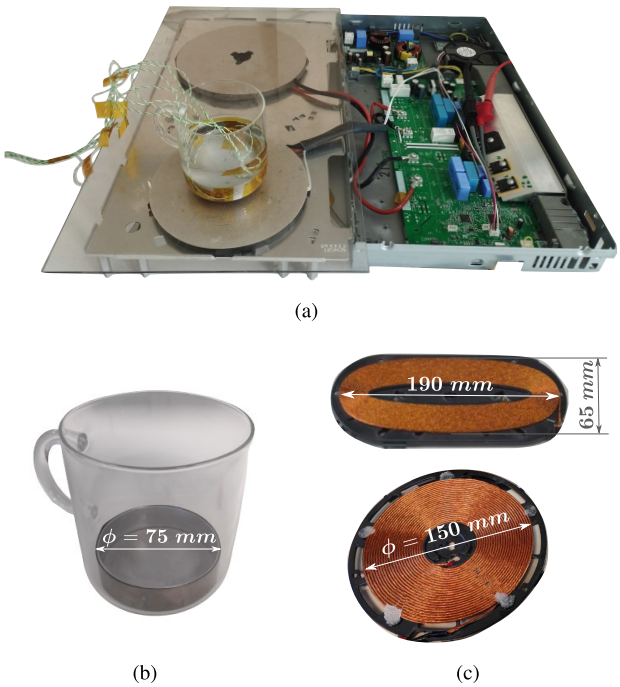

FIGURE 7. Experimental setup (a), inductive water heater prototype (b) and the elliptic, above, and circular, bellow, inductors used in the experimental measurements (c).

shown in Fig. 6, which corresponds to the experimental setup shown in Fig. 7(a). The prototype, shown in Fig. 7(b), has a diameter of 75 mm and a lateral wall of 20 mm. It consists of a bottom layer with 0.5 mm thickness made of the ferromagnetic alloy with low Curie temperature described in Section III-B and a top layer of 1 mm made of aluminum ($\mu_r = 1$ and $\sigma = 3.3 \cdot 10^7$ S/m). The mugs employed have the same diameter of 80 mm, and different height of the base (h_{mug}), varying between 3 mm, 5 mm, and 10 mm. The mugs are made of a material that is an electrical insulator, so it does not interfere with the induction heating process. Besides the material has low thermal conductivity (0.5 W/mK) which minimizes the thermal losses, since the lower this value, the higher the proportion of heat absorbed by the water. As for the inductors, it has been proved the adaptation of the water heater to the two different types of coils shown in Fig. 7(c). It has been tested in a circular inductor, as the one analyzed in Section III and an elliptical inductor, with the same type of cable as the other one and the dimensions shown in the figure. As for the relative position between inductor and load, the center of both have been placed in alignment, as shown in Fig. 7(a). Although the incorporation of the sidewalls allows the magnetic field to be attracted to the load reducing the adverse effects due to misalignment between the two elements, it is always recommended, as in any wireless power transfer application, that both elements be aligned to improve coupling.

A Lecroy MDA805A oscilloscope was used to acquire the voltage and current waveforms, which, conveniently post-processed, allow to obtain the equivalent circuit parameters (R_{eq} and L_{eq}). To measure the power consumed from the mains was employed a PM100 wattmeter. In addition, several thermocouples were used to obtain the temperature evolution in the water and the load, since infrared cameras are not suitable for measuring the temperature of a water mass because water behaves like a black body. Two experiments were conducted. The first one aims to test the performance of the load proposed for the water heater. It has been measured, at various frequencies, the R_{eq}, the L_{eq}, and the power in the inductor-load system. Based on the formulas described in Section II, the electrical efficiency at various frequencies has been calculated. It has also been proved that the PF varies when the temperature delimited by the Curie temperature of the load base material is exceeded, which allows to self-protect the system against overheating.

The second experiment compared the inductive heater with the microwave and kettle. A "Balay 3WGB2018 (800 W)" microwave oven and a "Bosch TWK3P420 (2200 W)" kettle were used. The test was performed with both at maximum power, and in the case of the inductive heater, it operated close the resonant frequency. For each, the power consumed, the preparation steps, the heating time, and the power transferred were obtained. The power transferred to the water P_{water} was calculated using the following relation:

$$E = mC_p\Delta T \tag{11}$$

$$P_{water} = \frac{E}{\Delta t} \tag{12}$$

where E is the thermal energy, m is the mass, C_p is the specific heat of the water, ΔT is the temperature increment, and Δt is the duration of the experiment in seconds. The tests have

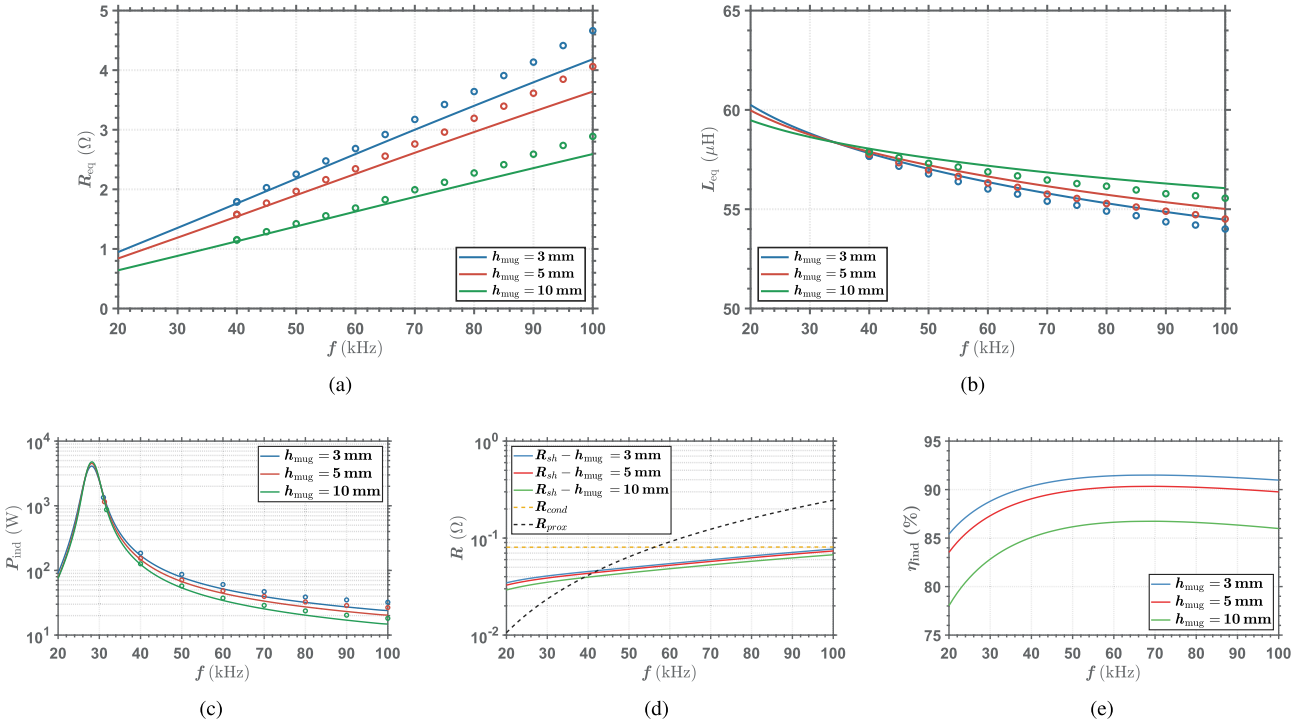

FIGURE 8. Performance at various frequencies of the equivalent resistance (a), equivalent inductance (b), power (c), losses (d) and electric efficiency of the inductor-load system (e) for the immersible load of 75 mm diameter and 20 mm h_{lat} with the circular inductor of 150 mm diameter.

been carried out with 300 ml of water, whose temperature has been increased from 25°C to 90°C to avoid the effects of evaporation and to facilitate the power calculation.

V. EXPERIMENTAL RESULTS

Fig. 8 shows the experimental (with dots) and simulated elements of the equivalent circuit for the immersible load used with the circular inductor. The study ranges from 20 kHz to 100 kHz, the usual operating frequency in domestic induction heating. Fig. 8(a) and Fig. 8(b) show the variation of the equivalent circuit parameters R_{eq} and L_{eq}, respectively, with the frequency when used in mugs with different base heights. As previously mentioned, when the h_{mug} increases, the equivalent resistance of the load decreases as the inductor-load distance increases. Fig. 8(c) shows the power that can be reached as a function of frequency. The simulation values have been obtained by analyzing the series resonant half-bridge inverter of the induction cooktop. Considering the R_{eq} values at frequencies close to resonance and that the cooktop components specifications recommend not exceeding an I_{rms} of 30 A, it can be supplied between 850 W and 1500 W depending on the height of the mug. Fig. 8(d) shows the losses calculated by FEM in the aluminum shielding (R_{sh}) and the losses in the winding, which are independent of the mug. Finally, Fig. 8(e) shows the electric efficiency of the inductor-load system. It can be observed that the efficiency increases with frequency, until 70 kHz where it starts to slowly decrease. This is caused by the fact that as the frequency increases, the power dissipated in the load increases in greater proportion than the losses. However, above 70 kHz, the proximity losses in windings, R_{prox}, start to become more relevant, causing the ratio between resistances and, therefore, the efficiency to decrease.

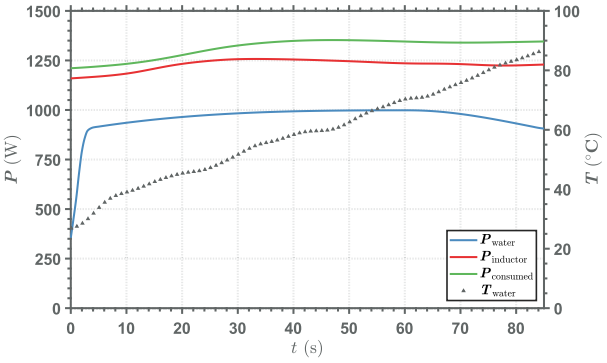

FIGURE 9. Experimental power measurements at $f = 31.5$kHz of the inductive heater with 300 ml of water.

Fig. 9 shows the power values obtained from a performance test of the inductive water heater in a mug with a base height of 5 mm and a circular inductor of 150 mm diameter at a frequency close to resonance (31.5 kHz). The power consumed from the mains was measured using the wattmeter and the input power to the inductor using the oscilloscope. By means of the water temperature evolution measured with the thermocouples and the Eq. 12, was estimated the power absorbed by

TABLE 1. Comparative results between the inductive water heater and other typical applications for domestic heating of liquids.

	MICROWAVE	KETTLE	INDUCTIVE HEATER	
			Ind. circular	Ind. elliptic
Total efficiency (%)	44.5	85.8	73.4	72.1
E_{cons}, per use (kWh)	0.051	0.026	0.029	0.030
$P_{demanded}$ (W)	1274	1884	1312	1263
P_{water} (W)	567	1616	964	911
Preparation steps	2	6	2	2
Heating time from 25-90°C of 300 ml water (s)	144	51	85	88
Additional comments	• Uneven temperature distribution	• Water overfilling • Longer preparation time	• Better results in inductors of similar load size	

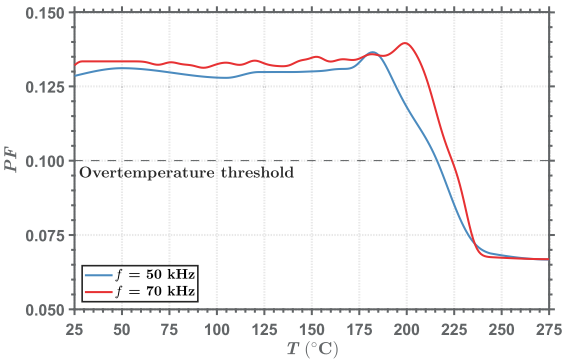

FIGURE 10. Experimental variation of the inductor-load system power factor with respect to temperature at different frequencies.

the water (P_{water}). Considering the power consumed and the total power absorbed to the water, a total efficiency (η_{tot}) of 73.4% was obtained. This efficiency includes the losses due to the induction cooktop electronics (rectifier stage, inverter), the losses in the inductor-load system,η_{ind}, as well as the losses of thermal origin since part of the heat is transferred to the mug, the environment and the ceramic glass among others. Fig. 10 shows the variation of the power factor (PF) with respect to the temperature of the load. This measure has been made without water inside the mug to allow the load to overheat. It can be observed that the PF drops clearly when the Curie temperature of the base material is exceeded, which is 230 °C. The $PF = 0.1$ is used as a threshold; below this value the power electronic converter is switched off protecting the system and the user.

The Table 1 compares the performance, at maximum power, between the microwave, the kettle, and the water heater used in different inductors. It also shows the number of manual steps involved in preparing hot water with each of them. In the case of the microwave, being an appliance that is always at hand in any kitchen, only two preparation steps are necessary: fill the cup with water and turn on the microwave. The inductive heater with the immersed load requieres the same steps: fill the cup with the heater embedded and turn on the induction cooktop. Finally, the kettle requires more preparation steps. First, it should be taken from storage and installed; second, it must be filled with water; third, it must be activated; fourth, the hot water must be poured into the mug; fifth, the kettle must be returned to the storage; finally, a sixth step is added which corresponds to the additional task of cleaning the kettle after each use.

From the table it can be extracted that the kettle is the one that transfers more energy to the water with better performance. However, it requires much longer preparation steps that make it uncomfortable for daily use, and, as mentioned above, it tends to be overfilled and part of the heated water is discarded, also causing a waste of energy. The microwave is more convenient in terms of preparation steps, but the temperature distribution in the water after being heated by this technology is not homogeneous making the infusion of poorer quality and also has low overall efficiency. Finally, the inductive heater combines both advantages: it is convenient to prepare and provides fast and efficient heating of the liquid inside. In addition, it takes up very little space. The results for the two types of inductors analyzed have been very similar, however, for the proper operation of the heater it is preferable to use it in inductors of similar size to the load.

VI. CONCLUSION

This paper proposes a water heater with an immersible load for domestic induction heating systems. It can be embedded or built into a ceramic mug and combines the convenience of the microwave with the temperature uniformity and efficiency of the kettle. The proposed load consists of a reduced diameter disk that incorporates lateral walls on the edge. This geometry allows it to be inserted, or be embedded into small vessels such as mugs, and to receive energy efficiently from induction cooktops with conventional inductors. The sidewalls provide a low reluctance path to the magnetic field, which increases the efficiency and the power transmitted to the load. However, to obtain fast and efficient heating of the liquid, it is advisable to be embedded in standard mugs without an excessively base height, since the increased distance to the inductor worsens the performance of the heating system. The performance and the power losses in the inductor-load system have been calculated by finite element analysis and measured experimentally with good agreement. Compared to traditional solutions such as microwave, it is more efficient and faster and obtains a homogeneous heat distribution

improving the final quality of the infusion. With respect to the kettle, it is easier to calculate the exact dosage of water, so it does not waste water and energy due to overfilling and is more convenient for daily use.

In this work, the technical feasibility of the inductive water heater has been studied, but there are still some points of improvement that could increase its competitiveness. For example, some product improvements include adding a cavity above the load to accommodate tea bags, or implementing the load geometry directly on the bottom of the mug.

REFERENCES

[1] L. Meng, K. W. E. Cheng, and K. W. Chan, "Systematic approach to high-power and energy-efficient industrial induction cooker system: Circuit design, control strategy, and prototype evaluation," *IEEE Trans. Power Electron.*, vol. 26, no. 12, pp. 3754–3765, Dec. 2011.

[2] I. Lope, J. Acero, and C. Carretero, "Analysis and optimization of the efficiency of induction heating applications with Litz-wire planar and solenoidal coils," *IEEE Trans. Power Electron.*, vol. 31, no. 7, pp. 5089–5101, Jul. 2016.

[3] A. Pascual, J. Acero, S. Llorente, C. Carretero, and J. M. Burdio, "Self-adaptive overtemperature protection materials for safety-centric domestic induction heating applications," *IEEE Access*, vol. 11, pp. 1193–1201, 2023.

[4] J. Acero, J. Burdío, L. Barragán, D. Navarro, R. Alonso, J. García, F. Monterde, P. Hernández, and S. L. I. Garde, "Domestic induction appliances," *IEEE Ind. Appl. Mag.*, vol. 16, no. 2, pp. 39–47, Mar. 2010.

[5] O. Lucia, J. Acero, C. Carretero, and J. M. Burdio, "Induction heating appliances: Toward more flexible cooking surfaces," *IEEE Ind. Electron. Mag.*, vol. 7, no. 3, pp. 35–47, Sep. 2013.

[6] O. Lucia, D. Navarro, P. Guillén, H. Sarnago, and S. Lucia, "Deep learning-based magnetic coupling detection for advanced induction heating appliances," *IEEE Access*, vol. 7, pp. 181668–181677, 2019.

[7] W. Han, K. T. Chau, C. Jiang, and W. Liu, "All-metal domestic induction heating using single-frequency double-layer coils," *IEEE Trans. Magn.*, vol. 54, no. 11, pp. 1–5, Nov. 2018.

[8] J. Acero, I. Lope, C. Carretero, and J. M. Burdio, "Adapting of non-metallic cookware for induction heating technology via thin-layer non-magnetic conductive coatings," *IEEE Access*, vol. 8, pp. 11219–11227, 2020.

[9] A. Pascual, J. Acero, J. M. Burdío, C. Carretero, and S. Llorente, "Electrothermal analysis of temperature-limited loads for domestic induction heating applications," in *Proc. 48th Annu. Conf. IEEE Ind. Electron. Soc. (IECON)*, Oct. 2022, pp. 1–6.

[10] M. Huang, C. Liao, Z. Li, Z. Shih, and H. Hsueh, "Quantitative design and implementation of an induction cooker for a copper pan," *IEEE Access*, vol. 9, pp. 5105–5118, 2021.

[11] O. Lucia, P. Maussion, E. J. Dede, and J. M. Burdio, "Induction heating technology and its applications: Past developments, current technology, and future challenges," *IEEE Trans. Ind. Electron.*, vol. 61, no. 5, pp. 2509–2520, May 2014.

[12] S. Llorente, F. Monterde, J. M. Burdío, and J. Acero, "A comparative study of resonant inverter topologies used in induction cookers," in *Proc. 17th Annu. IEEE Appl. Power Electron. Conf. Expo.*, Mar. 2002, pp. 1168–1174.

[13] G. H. Brown, C. N. Hoyler, and R. A. Bierwirth, *Theory and Application of Radio-Frequency Heating*. New York, NY, USA: Van Nostrand, 1947.

[14] P. Vishnuram, G. Ramachandiran, T. S. Babu, and B. Nastasi, "Induction heating in domestic cooking and industrial melting applications: A systematic review on modelling, converter topologies and control schemes," *Energies*, vol. 14, no. 20, p. 6634, Oct. 2021.

[15] D. Kim, J. So, and D. Kim, "Study on heating performance improvement of practical induction heating Rice cooker with magnetic flux concentrator," *IEEE Trans. Appl. Supercond.*, vol. 26, no. 4, pp. 1–4, Jun. 2016.

[16] E. Plumed, I. Lope, J. Acero, and J. M. Burdío, "Domestic induction heating system with standard primary inductor for reduced-size and high distance cookware," *IEEE Trans. Ind. Appl.*, vol. 58, no. 6, pp. 7562–7571, Nov. 2022.

[17] "At home with water," Energy Saving Trust, London, U.K., Tech. Rep. 1, 2013. [Online]. Available: https://www.energysavingtrust.org.uk/sites/default/files/reports/AtHomewithWater%287%29.pdf

[18] D. M. Murray, J. Liao, L. Stankovic, and V. Stankovic, "Understanding usage patterns of electric kettle and energy saving potential," *Appl. Energy*, vol. 171, pp. 231–242, Jun. 2016.

[19] P. Zhao, W. Gan, C. Feng, Z. Qu, J. Liu, Z. Wu, Y. Gong, and B. Zeng, "Multiphysics analysis for unusual heat convection in microwave heating liquid," *AIP Adv.*, vol. 10, no. 8, Aug. 2020, Art. no. 085201.

[20] S. Lakshmi, A. Chakkaravarthi, R. Subramanian, and V. Singh, "Energy consumption in microwave cooking of Rice and its comparison with other domestic appliances," *J. Food Eng.*, vol. 78, no. 2, pp. 715–722, Jan. 2007.

[21] E. Plumed, I. Lope, and J. Acero, "Induction heating adaptation of a different-sized load with matching secondary inductor to achieve uniform heating and enhance vertical displacement," *IEEE Trans. Power Electron.*, vol. 36, no. 6, pp. 6929–6942, Jun. 2021.

[22] E. Plumed, I. Lope, and J. Acero, "Modeling and design of cookware for induction heating technology with balanced electromagnetic and thermal characteristics," *IEEE Access*, vol. 10, pp. 83793–83801, 2022.

[23] J. Acero, C. Carretero, R. Alonso, and J. M. Burdio, "Quantitative evaluation of induction efficiency in domestic induction heating applications," *IEEE Trans. Magn.*, vol. 49, no. 4, pp. 1382–1389, Apr. 2013.

[24] J. Acero, R. Alonso, J. M. Burdío, L. A. Barragán, and D. Puyal, "Frequency-dependent resistance in Litz-wire planar windings for domestic induction heating appliances," *IEEE Trans. Power Electron.*, vol. 21, no. 4, pp. 856–866, Jul. 2006.

[25] C. Carretero, I. Lope, and J. Acero, "Magnetizable concrete flux concentrators for wireless inductive power transfer applications," *IEEE J. Emerg. Sel. Topics Power Electron.*, vol. 8, no. 3, pp. 2696–2706, Sep. 2020.

[26] C. Carretero, J. Acero, and R. Alonso, "TM-TE decomposition of power losses in multi-stranded Litz-wires used in electronic devices," *Prog. Electromagn. Res.*, vol. 123, pp. 83–103, 2012.

[27] E. Plumed, I. Lope, and J. Acero, "EMI reduction via resonator coils in glassless integrated domestic induction systems," *IEEE Access*, vol. 9, pp. 128147–128156, 2021.

[28] *2005 Measurement Methods for Electromagnetic Fields of Household Appliances and Similar Apparatus With Regard to Human Exposure*, Standard IEC 62233, 2005. [Online]. Available: https://cir.nii.ac.jp/crid/1571980076076221184

[29] D. Paesa, C. Franco, S. Llorente, G. López-Nicolás, and C. Sagüés, "Adaptive simmering control for domestic induction cookers," *IEEE Trans. Ind. Appl.*, vol. 47, no. 5, pp. 2257–2267, Sep. 2011.

[30] A. Pascual, J. Acero, C. Carretero, and S. Llorente, "Experimental characterization of materials with controlled Curie temperature for domestic induction heating applications," in *Proc. 47th Annu. Conf. IEEE Ind. Electron. Soc. (IECON)*, Oct. 2021, pp. 1–6.

[31] A. Pascual, J. Acero, J. M. Burdìo, S. Llorente, and C. Carretero, "Self-protection systems for domestic induction heating based on ferromagnetic materials with low Curie temperature," in *Proc. IEEE 31st Int. Symp. Ind. Electron. (ISIE)*, Jun. 2022, pp. 314–319.

[32] A. Bono-Nuez, B. Martin-del-Brio, C. Bernal-Ruiz, F. J. Perez-Cebolla, A. Martinez-Iturbe, and I. Sanz-Gorrachategui, "The inductor as a smart sensor for material identification in domestic induction cooking," *IEEE Sensors J.*, vol. 18, no. 6, pp. 2462–2470, Mar. 2018.

[33] J. Villa, D. Navarro, A. Dominguez, J. I. Artigas, and L. A. Barragan, "Vessel recognition in induction heating appliances—A deep-learning approach," *IEEE Access*, vol. 9, pp. 16053–16061, 2021.

ALBERTO PASCUAL (Graduate Student Member, IEEE) received the M.Sc. degree in electronic systems engineering from the Polytechnic University of Madrid, Spain, in 2016, and the degree in industrial technologies engineering from the University of Zaragoza, where he is currently pursuing the Ph.D. degree. He is a member of Instituto de Investigación en Ingeniería de Aragón (I3A), Power Electronics and Microelectronics Group (GEPM). His research interests include the analysis and development of advanced technologies for induction heating focused on self-protection.

JESÚS ACERO (Senior Member, IEEE) received the M.Sc. and Ph.D. degrees in electrical engineering from the University of Zaragoza, Zaragoza, Spain, in 1992 and 2005, respectively. From 1992 to 2000, he worked in several industry projects, especially focused on custom power supplies for research laboratories. Since 2000, he has been with the Department of Electronic Engineering and Communications, University of Zaragoza, Spain, where he is currently a Professor. His research interests include resonant converters for induction heating applications, inductive-type load modeling, and electromagnetic modeling. He is a member of the IEEE Power Electronics, Industrial Electronics and Magnetics Societies. He is also a member of Instituto de Investigación en Ingeniería de Aragón (I3A).

SERGIO LLORENTE received the M.Sc. and Ph.D. degrees in electronic engineering from the University of Zaragoza, Zaragoza, Spain, in 2001 and 2016, respectively. In 2001, he joined Bosch-Siemens Home Appliances Group, Zaragoza, where he has held different positions with the Research and Development Department, Induction Cooktops. He is currently an in charge of several research lines and preprojects, and also an inventor in more than 200 patents. He has also been an Assistant Professor with the University of Zaragoza, since 2004. His research interests include power electronics, simulation and control algorithms for power electronics, and temperature.

CLAUDIO CARRETERO (Senior Member, IEEE) received the B.Sc. and M.Sc. degrees in physics, the B.Sc. and M.Sc. degrees in electrical engineering, and the Ph.D. degree in electrical engineering from the University of Zaragoza, Zaragoza, Spain, in 1998, 2002, and 2010, respectively. He is currently an Assistant Professor with the Department of Applied Physics, University of Zaragoza. His research interests include induction heating applications and the electromagnetic modeling of inductive systems. He is a member of Instituto de Investigación en Ingeniería de Aragón (I3A).

JOSÉ M. BURDIO (Senior Member, IEEE) received the M.Sc. and Ph.D. degrees in electrical engineering from the University of Zaragoza, Zaragoza, Spain, in 1991 and 1995, respectively. He has been with the Department of Electronic Engineering and Communications, University of Zaragoza, where he is currently a Professor, the Head of the Group of Power Electronics and Microelectronics, and the Director of the BSH Power Electronics Laboratory, University of Zaragoza. In 2000, he was a Visiting Professor with the Center for Power Electronics Systems, Virginia Tech. He is the author of more than 80 international journal articles and over 200 papers in conference proceedings and the holder of more than 60 international patents. His research interests include the modeling of switching converters and resonant power conversion for induction heating and biomedical applications. He is a Senior Member of the Power Electronics and Industrial Electronics Societies. He is also a member of Instituto de Investigación en Ingeniería de Aragón (I3A).